

INVESTIGATION OF BRAIN ARTERIAL CIRCLE MALFORMATIONS USING ELECTRICAL MODELLING AND SIMULATION

K. Čáková, V. Blazek, I. Čáp

*University of Zilina, Faculty of Electrical Engineering, Velký diel, 010 26 Zilina, Slovakia
Tel.: +421-41-513 2100, Fax: +421-41-513 1519, E-mail: capova@fel.utc.sk*

Summary: The paper deals with the cerebral arterial system investigation by means of electrical modelling and simulations. The main attention is paid to the brain arterial circle malformations (stenoses and aneurysms) and their determination and evaluation by computer-aided methods as tools of a non-invasive diagnostics. The compensation possibilities of brain arterial circle in case of presence of concrete arterial malformations are modelled and simulated. The simulation results of brain arteries blood pressures and volume flow velocities time dependences are presented and discussed under various health conditions.

Keywords: brain arterial circle, arterial malformation, electromechanical analogy, electrical modelling and simulations, non-invasive diagnostics, computer-aided methods, state variables.

1. INTRODUCTION

During the medical treatment of cerebro-vascular diseases it is often necessary to occlude one of the brain supplying arteries. Due to the arterial circle of Willis (CAW – Circulus Arteriosus Willisii) this intervention contains no further consequences for the majority of patients. But because of an unfavourable vessel anatomy or vessel disease this intervention causes an ischemia in corresponding parts of the brain for some patients who then may suffer from strokes.

Until now, this situation can only be estimated by invasive and inaccurate diagnostics, which themselves contain the risk of cerebro-vascular accidents.

For this reason profound insights into the complex haemodynamic interactions within the brain were tried to enable by modelling the arterial circle of Willis. Replacing invasive diagnostics by computational simulations, a reliable and non-invasive diagnostic tool estimating the haemodynamic effects of endovascular vessel occlusion is obtained. The model is based upon the analogy of hydrodynamic and electromagnetic state variables called as electromechanical analogy, [1], [2], [3].

The vessel properties are described by coupled first order linear differential equations, which are subsequently nonlinearly extended. The anatomical parameters and boundary conditions of the differential equations are defined by non-invasive, clinically established diagnostics. By these means any given anatomical structure of vessels can be designed. Time continuous simulations of different states of all calculated state variables, such as blood pressure and flow in any given vessel of the model,

become feasible and online observable. Critical occlusions can be simulated and corresponding changes in flow or pressure can be observed without exposing the patient to a risk of health, [4] to [7].

On the first stage of development the individual model of each patient must be designed and validated by a comparison with measured data. Although an agreement between the modelled data and those recorded from observation of the subjects is not reached in each case, because the state variables generated by the model behave physiologically. The reaction of individual cerebro-vascular systems in critical situations as occlusions of the main brain arteries is investigated under special conditions. Some deviations between modelled and measured data are based on systematic inaccuracies concerning the determination of the vessels geometry.

Using the mentioned electromechanical analogy the equivalent electromagnetic systems have been derived and consequently the computer modelling and simulation of CAW under various conditions were performed. The results of the CAW equivalent electromagnetic systems derivation and their modelling and simulations were published in the previous works [6], [7], [8]. Following from these works the CAW significant malformations have been investigated and evaluated by means of the electrical modelling and simulations in this paper.

2. THEORY

The standard model of CAW is the main basis for the individual modelling of vessels networks of individual patients CAW. The principal topology of CAW is illustrated at Fig.1.

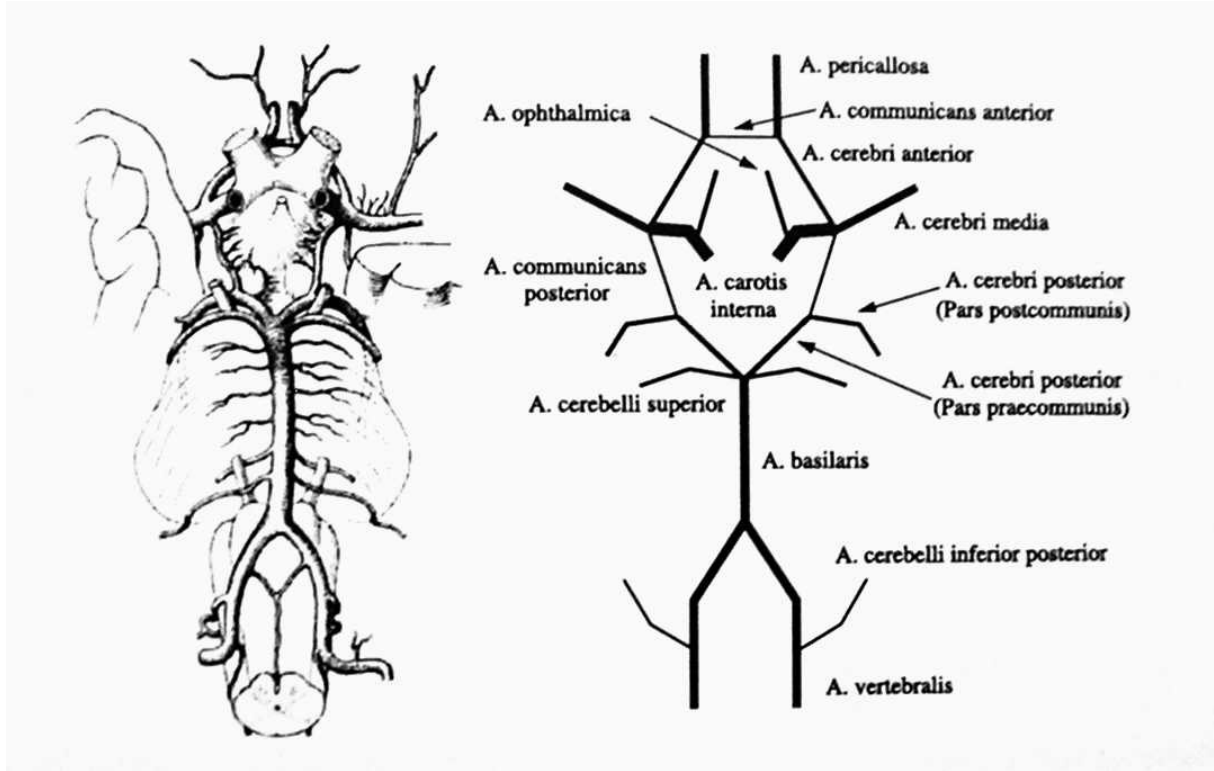


Fig. 1. Topology of brain arterial system

The basic equations of one vessel segment modelled by the equivalent electric two-port element according to the electromechanical analogy are expressed in

$$Z_i(t) = \int_0^t \frac{1}{L_i(t)} [P_{i-1}(t) - P_i(t) - I_i(t)R_i(t)]dt + I_i(0) \quad (1)$$

$$P_i(t) = \frac{2}{3} \rho l^2 \left(\frac{I_i(t)}{Q_i(t)} \right)^2 + R_{di} [I_i(t) - I_{i+1}(t)] + \frac{Q_i(t) - Q_{iu}}{C_i(t, \omega)} + P_{ex.}(t) \quad (2)$$

$$Q_i(t) = \int [I_i(t) - I_{i+1}(t)]dt + Q_i(0), \quad (3)$$

where I_i is the blood flow, P_i blood pressure and Q_i blood volume in the i -th vessel segment, R_i is a viscose friction resistance of flowing blood and R_{di} resistance corresponding to the friction losses inside the vessel wall of segment i .

The vessels parameters in i -th vessel segment, resistance R_i and inductance L_i in longitudinal direction and the capacitance C_i and cross-conductance G_i in transversal direction, depend on the vessel geometry and the elasticity of vessel walls. The formulas enabling their calculations are given, by following expressions, [2] and [3]

$$R_i(t) = \frac{8\eta l_i}{\pi r_i^4(t)}, \quad C_i(t, \omega) = \frac{3}{2} \frac{\pi l_i}{E_{di}(\omega) h_i(t)} \frac{r_{0i}^5}{r_i^2(t)}$$

$$L_i(t) = \frac{\rho l_i}{\pi r_i^2(t)}, \quad R_{di}(t) = \frac{2}{3} \frac{\eta_{0i}(t) h_i(t)}{\pi r_{0i}^3 l_i}, \quad (4)$$

terms of the haemodynamic state values in differential equations, [4], [5]

where η is the blood viscosity, l_i is the length of a vessel segment i , r_i vessel internal radius, r_0 the vessel internal radius without drawing out, ρ is the blood density, E_{di} is the relative dynamic part of Young elasticity modulus, h_i is the vessel wall thickness of segment i .

From the preoperative CAW risk estimation point of view there is the realistic simulation of the arterial malformations, especially stenoses, of the main importance in this area. In order to investigate the influences of an arterial stenosis in terms of the state values as blood pressure or blood velocity, the basic mathematical model, (e.g. in [6]), should be aided by the equation expressing the mutual continuity between the pressure drop caused by the stenosis and the blood flow through the vessel section under stenosis influence,

$$\Delta P_{stenose}(t) = \frac{\eta K_v}{2\pi r^3(t)} I(t) + \frac{\rho K_t}{2\pi^2 r_0^4} \left(\frac{r_0^2}{r_{st}^2} - 1 \right)^2 |I(t)| I(t) + \frac{\rho l_{st} K_u}{\pi r^2(t)} \frac{dI(t)}{dt}, \quad (5)$$

in which the $r(t)$ is the internal radius of the vessel (pipe) run through by blood, r_0 the internal radius in the healthy vessel and r_{st} the internal radius in the place of the highest stenosis (which means maximum narrowing of the vessel).

The length of the stenosis is described by l_{st} , η and ρ design the blood viscosity and density correspondingly. The coefficients K_t , K_u and K_v were stated empirically, [5]. The shape (profile) of the stenosis has been described by the cosinus function

$$r(x) - r_0 = -f(x), \text{ where } f(x) = \frac{\delta}{2} \left[1 + \cos\left(\frac{2\pi x}{l_{st}}\right) \right]$$

$$\text{and } x = \left[-\frac{l_{st}}{2}, \frac{l_{st}}{2} \right] \quad (6)$$

The δ is the maximum height of the stenosis, Fig. 2. The stenosis parameters for the simulation are also given at the Fig.2. The nonlinearities caused by blood whirl, eq. (1), create the main reason for the intensified pressure drop in the vessel under stenosis influence.

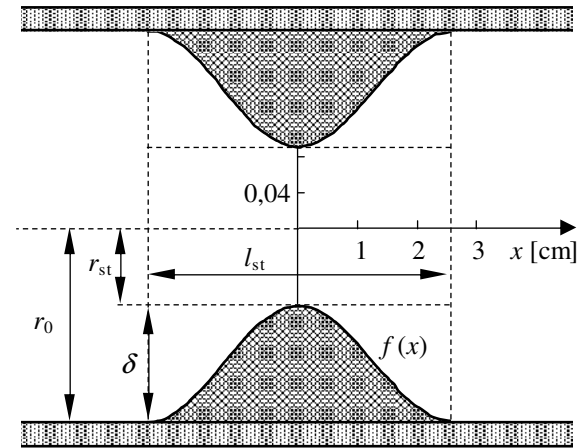


Fig. 2. Vessel segment with stenosis.

According to the previous works the following stenosis parameters of the equivalent electric system of the vessel segment can be defined by the relations

$$L_{st}(t) = \frac{\rho l_{st} K_u}{\pi r^2(t)}, \quad R_{st}(t) = \frac{\eta K_v}{2\pi r^3(t)}, \quad R_{dp}(t) = \frac{\rho K_t |I(t)|}{2\pi^2 r_0^4} \left(\frac{r_0^2}{r_{st}^2} - 1 \right)^2 \quad (7)$$

Then the equation (5) can be expressed by relations

$$\Delta P_{stenose}(t) = [R_{st}(t) + R_{dp}(t)]I(t) + L_{st}(t) \frac{dI(t)}{dt}$$

$$I(t) = \int \frac{1}{L_{st}(t)} [\Delta P_{stenose}(t) - I(t)(R_{st}(t) + R_{dp}(t))] dt + I(0) \quad (8)$$

The resistance $R_{st}(t)$ is similar to the stationary longitudinal resistance in Hagen - Poiseuille law, [1], and it expresses the fact that with the increasing a vessel narrowing the viscose friction also grows up. Its value is strongly influenced by the stenosis geometry. The coefficient K_v is no more constant, but it is a function dependent on the stenosis shape. The term R_{dp} describes the resistance which arises

under the influence of the poststenotic turbulences and it depends only a little on the stenosis geometry. The equation (8) is the equivalent one to the differential equation (5), which describes the blood state values of a vessel segment without stenosis. In the case of a vessel segment with the stenosis i the following differential equation is used for the blood flows calculations

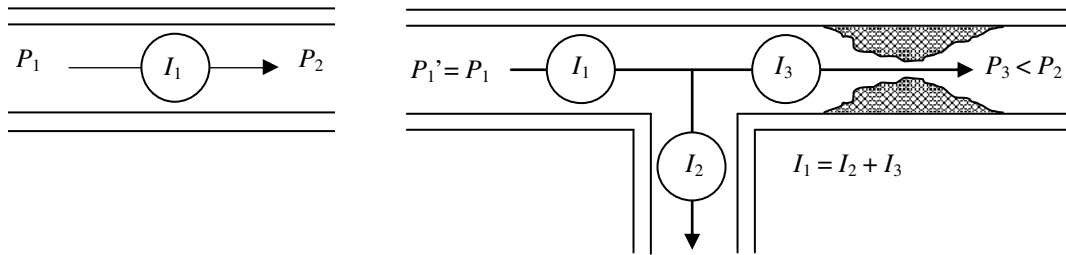
$$I_i(t) = \int \frac{1}{L_{st}(t)} [P_{i-1}(t) - P_i(t) - I_i(t)(R_i(t) + R_{st}(t) + R_{dp}(t))] dt + I_i(0), \text{ with } R_i(t) = \frac{8\eta l_i}{\pi r_i^4(t)} \quad (9)$$

By the value L_{st} the effect of the blood inertial mass has been involved into the calculations.

In order to respect better the stenosis influence on the CAW haemodynamics the stenosis degree SD has been considered. The formula for the SD determination is

$$SG = \left(1 - \frac{A_{st}}{A_0} \right) \times 100 = \left(1 - \frac{r_{st}^2}{r_0^2} \right) \times 100 \quad (10)$$

where A_0 is the healthy vessel cross-section and A_{st}



is the cross-section of the vessel under the stenosis. For the modeling reasons the stenosis has been placed in the Arteria carotis interna, concretely 5 cm above the splitting of Arteria carotis communis in the Arteria carotis interna and externa, Fig.1. The input

signal has been created by blood flow velocities in the right Arteria vertebralis and the left Arteria carotis interna.

The stenosis model is given at Fig. 3, where the modeled prestenotic vessel shunt is shown.

Fig.3. Topology of the modelled prestenotic shunt.

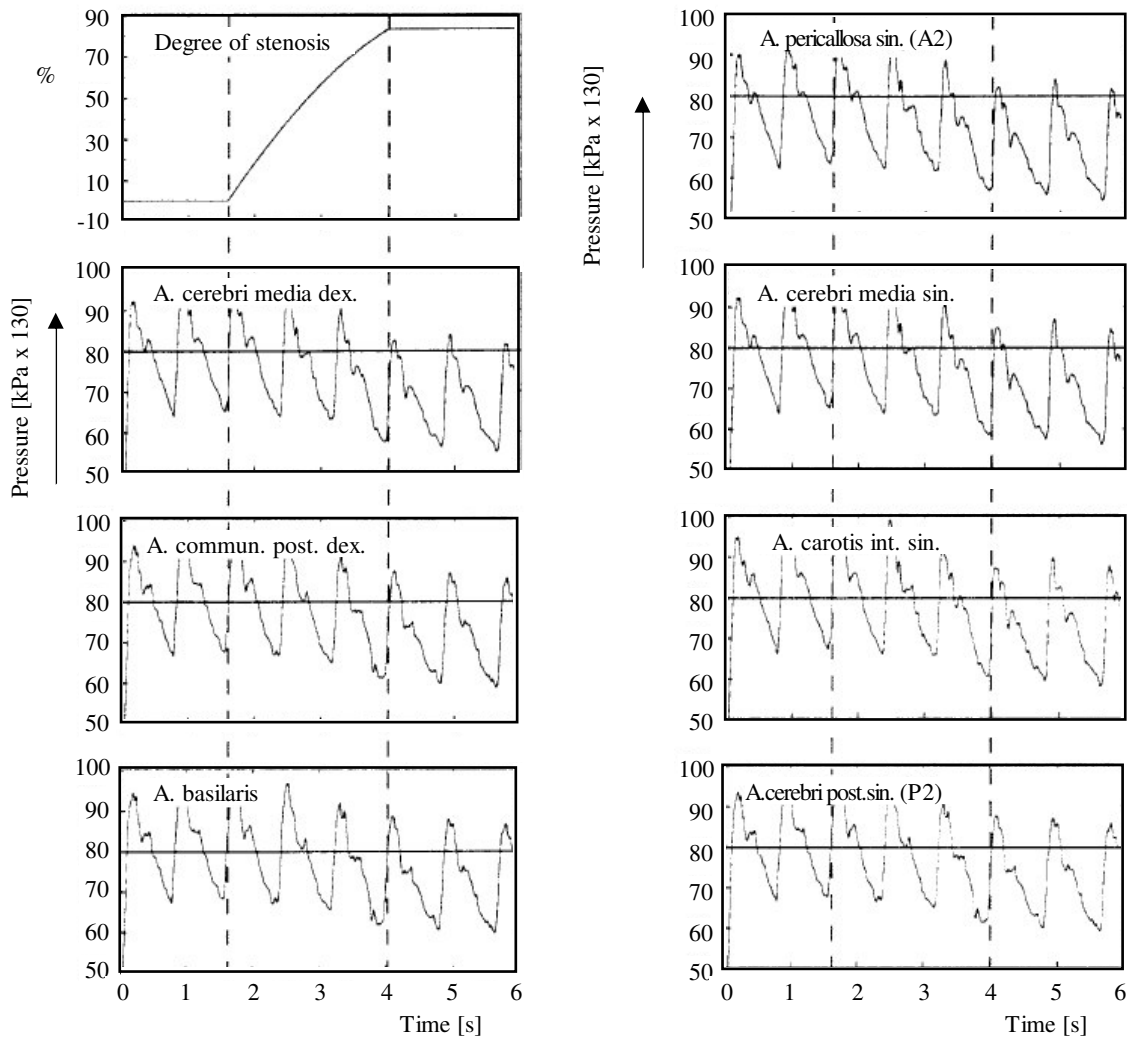


Fig. 4. The blood pressure time dependence in CAW in the case of stenosis in Arteria Carotis Interna

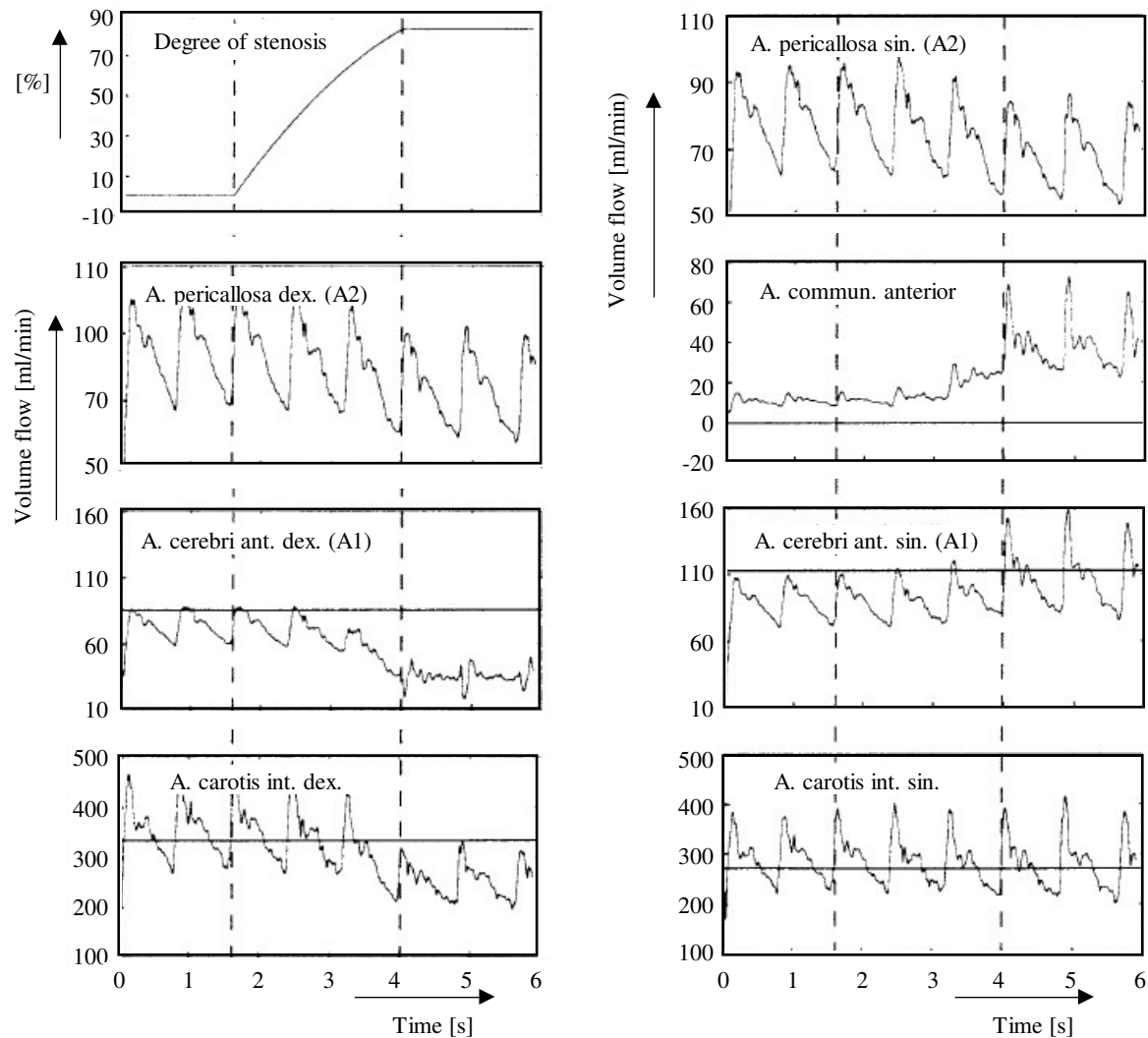


Fig. 5. The blood flow time dependence in CAW in the case of stenosis in Arteria Carotis Interna.

Because of stenosis the reduced blood flow I leaves the prestenotic vessel part ($I_3 < I_1$). In order to keep the continuity principle the aided blood flow I_2 leaves the modeled vessel segment through the shunt. The blood pressure in the prestenotic part hardly increases while the considerable pressure drop P in the poststenotic vessel part is remarkable ($P_3 < P_2$). In the principle the flow I_2 corresponds to a prestenotic blood roundabout way into other vessels, in this case benefit to Arteria carotis externa or Arteria subclavia and it leads to a less congestion of the poststenotic areas.

3. RESULTS

The following simulation results according to the CAW topology, Fig. 1, and with a slowly continuous increase of stenosis degree are presented in Fig. 4 and Fig. 5. The graphs represent the blood pressure and blood flow time dependences in various intracranial arteries (of CAW).

The vessel segment (Arteria carotis interna sinistra)

parameters, [4], [5], used for the simulation are given by following way, radius $r_0 = 0,192\text{cm}$, length $l = 5\text{cm}$, elasticity $E_l = 1,1652 \times 10^6 \text{ g/cm.s}^2$ and pulse wave velocity $\text{PWV} = 925\text{cm/s}$. The maximum stenosis degree was $\text{SG}_m = 83\%$, the stenosis length was $l_{st} = l = 5\text{cm}$. The mean arterial pressure corresponds in all vessels before the stenosis introduction to the mean pressure values given in the literature, [4], [5], Fig. 1.

In the case of blood pressure the significant changes occur as far as the stenosis degree value is about 70%. The small blood pressure drop is by the reduced congestion in the CAW evident and in accordance with the principle of continuous pipes the pressure drop in all other vessels is also possible to explain.

Also in the case of blood flow, a nonlinear part of the whole resistance R_{dp} becomes more important than the linear one R_{st} mainly with the growth of the stenosis degree. The most distinct is the reducing of the blood flow in the right Arteria carotis interna behind the stenosis, while the flow in the left Arteria

carotis interna is nearly the same in spite of the stenosis, Fig. 2. From the Fig. 2 there is possible to show the CAW as the responsible and reliable one for the vascularization of the brain. The simulation results show how because of stenosis in one vessel segment the flow distribution in CAW develops in order to ensure a sufficient blood supply of the brain. In the left Arteria cerebri anterior (A1) the blood flow increases so that not only the left one but also the right (A2) through the Arteria communicans anterior is supplied by blood. Simultaneously the blood flow in the A1 decreases and so significantly more blood can flow from the stenotic Arteria carotis interna into the right Arteria cerebri media.

4. CONCLUSION

The obtained simulation results for the blood pressure and mainly for the blood flow show the compensation possibilities of CAW in case of one brain arterial occlusion. The critical occlusions of an individual cerebral model were simulated and corresponding changes in flow and pressure were observed without exposing the patient to a risk of health. The reactions of the individual arterial system in critical situations were investigated and compared with the recorded data from observations of the subject. The elaborated method of a non/invasive preoperative risk/estimation can be assessed to be efficient. There is hope that this flexible, time saving and reproducible method makes a valuable contribution to avoid complications of induced vessel occlusion during medical treatment by an improved operation planning.

REFERENCES

- [1] Jager, G. N., Westerhof, N., Noordergraaf, A.: Oscillatory Flow Impedance in Electrical Analogy of Arterial System, *Circulation Research* 16 (1965), 121-133.
- [2] Gaelings, E.W.: Numerische Simulation Haemodynamischer Prozesse in Vascularen Netzen, Shaker Verlag Aachen, 1996, ISBN-3-8265-1509-9.
- [3] Čáková, K., Blazek, V., Čáp, I., Bučkuliaková, L.: Physiological Fluid System Modelling and Visualization, *International Journal of Applied Electromagnetics and Mechanics*, 14 (2002), IOS Press, pp.377/380.
- [4] Hillen, B., Hoogstraten, H.V., Rost, L.: A Mathematical Model of the Flow in the Circle of Willis, *Journal of Biomechanics* 19 (1986), No.3, pp. 187-195.
- [5] Roessler, F.C.: Entwicklung eines computergestützten Simulationsverfahrens zur preoperativen, nichtinvasiven Risikoabschätzung bei zerebralen Gefäßeingriffen, *Fortschritt Berichte VDI*, VDI Verlag, GmbH Düsseldorf, 2005.
- [6] Čáková, K., Čáp, I., Blazek, V.: Brain haemodynamics modelling using electromagnetic systems characteristics, *International Journal of Applied Electromagnetics and Mechanics* 19 (2004), IOS Press, pp. 457-462.
- [7] Čáková, K., Blazek, V., Čáp, I.: Pathological Deformations of Brain Vascular System Modelling using Analogous Electromagnetic Systems, *Advances in Electrical and Electronic Engineering*, No. 2, Vol. 3, 2004, pp. 213-216.
- [8] Viedma, A., Ortiz, C.J., Marco, V.: Extended Willis circle model to explain clinical observations in periorbital artery, *Journal of Biomechanics*, 30 (1997), pp. 265-272